**Journal of Magnetics** 14(1), 1-6 (2009)

# Magnetic Property of $Bi_xCa_{1-x}MnO_3$: Experimental and First Principles Calculation Study

**Sung-Ho Na* and Dong-Jin Kim**

*Department of Physics/RCDAMP, Pusan National University, Pusan 609-735, Korea*

(Received 23 October 2008, Received in final form 27 November 2008, Accepted 1 December 2008)

**The magnetic properties of $Bi_xCa_{1-x}MnO_3$ for x = 0.12, 0.13, 0.14, 0.15, and 0.16 were examined by measuring magnetic susceptibility, resistivity and electron magnetic resonance at different temperatures. $Bi_xCa_{1-x}MnO_3$ showed complicated magnetic structure that varies with temperature and composition, particularly around Bi composition x ≈ 0.15. The aim of this study was to determine how the magnetic and physical properties of $Bi_xCa_{1-x}MnO_3$ change in this region. In addition, first principles calculations of the magnetic phase of $Bi_xCa_{1-x}MnO_3$ for x = 0, 0.125, 0.25 were carried out, and the spin state, electric and magnetic characteristics are discussed.**

**Keywords :** $Bi_xCa_{1-x}MnO_3$, susceptibility, density functional theory, electron magnetic resonance, resistivity

## 1. Introduction

$Bi_xCa_{1-x}MnO_3$ is a highly correlated perovskite manganite that has been reported to exhibit complicated phase changes [1-4]. The magnetic susceptibility of $Bi_xCa_{1-x}MnO_3$ shows large variation with changes in both temperature and composition. Although there have been some experimental investigations, the intervals of their sample composition was approximately 5~10%. Therefore, a more thorough investigation would be necessary for a better understanding.

Five polycrystalline samples of $Bi_xCa_{1-x}MnO_3$ with x = 0.12, 0.13, 0.14, 0.15, and 0.16 were synthesized and characterized by measuring their magnetic susceptibility, electron magnetic resonance (EMR) and resistivity. $Bi_xCa_{1-x}MnO_3$ exhibited charge ordering at Bi content down to 0.14. The charge ordering temperature in that limiting composition ($Bi_{0.14}Ca_{0.86}MnO_3$) was found to be 152 K. The resistivity of $Bi_xCa_{1-x}MnO_3$ increases with increasing Bi content and changes over a certain temperature range. For samples with Bi content x = 0.13 and 0.15, this temperature is near their Neel temperatures. The EMR line-width decreases with decreasing temperature, and this temperature dependence matches with the resistivity measurements.

*Corresponding author: Tel: +82-51-510-1769
Fax: +82-51-513-7664, e-mail: sunghona@pusan.ac.kr

First principles calculations of $Bi_xCa_{1-x}MnO_3$ for x = 0, 0.125, and 0.25 (also 0.5, 0.75, and 1) were performed to determine the total energy of a unit cell, electronic density of states and the magnetic moment of atoms in different magnetic phases. The relative stability between the different magnetic phases was determined by comparing the calculated total energy. The resistivity was also considered by the calculated density of states. Anti-ferromagnetic phases are generally confirmed for $Bi_xCa_{1-x}MnO_3$ with various Bi contents. However, different calculation methods, as LSDA and LSDA+U (LSDA: local spin density approximation, LSDA+U = LSDA + on site Coulomb interaction), make different predictions of the most stable magnetic phase [5, 6].

## 2. Experiment and First Principles Calculation

Samples were prepared using the standard solid reaction method. A correct stoichiometric mixture of $MnO_2$, $Mn_2O_3$, $CaCO_3$, and $Bi_2O_3$ was calcined at 700 °C for 20 hours. The $CaCO_3$ and $Bi_2O_3$ were preheated to 150 °C for a few hours prior to calcination to remove all moisture, which could hinder correct weighing. The inclusion of $Mn_2O_3$ sets the average valence of manganese ions in the mixture to the one desired in the final samples. After calcination, the mixture was ground and reacted in air at 1050 °C for 18 hours. This reaction process was repeated once more.

The resulting material was reground and pressed into a one inch, 3 mm thick pellet. Sintering is carried in air at 1080 °C for 48 hours. Because bismuth tends to evaporate during the reaction process, 20% and 10% excess of $Bi_2O_3$ were added before the two each successive reaction processes, respectively. XRD and ICP analysis showed no notable bismuth deficiency in these samples.

X-ray diffraction (XRD, $\theta$–$2\theta$) was performed for each sample under the following measurement conditions: Cu target, $\lambda = 1.5406$A, continuous scan with a speed of 2.00 deg/min, 40 kV, 30 mA, divergence slit angle = 1.00 deg, scatter slit angle = 1.00 deg, an receiving slit width = 0.30 mm. A superconducting quantum interence device (SQUID) was used to measure the induced magnetization of each sample at temperatures ranging from approximately 5~300 K. Two distinct applied magnetic fields were used, 100 Oe and 3000 Oe. A continuous wave EMR experiment was carried out for each sample in the cavity under temperature control using a cool nitrogen gas flow. The magnetic field sweep range was 0~0.7 Tesla. The resistivity of the two samples with Bi content of x = 0.13 and 0.15 were measured using a current source meter (Keithley 237, USA) for temperature ranging from 60 to 300 K.

First principles calculations based on density functional theory were carried out to identify the most stable magnetic phase for each $Bi_xCa_{1-x}MnO_3$ with x = 0, 0.125, 0.25, 0.5, 0.75, and 1 to identify the density of states and spin magnetic moments. The ferromagnetic state and three major anti-ferromagnetic states, A type, G type, and C type, were considered.

## 3. Result and Discussion

Fig. 1 shows the XRD pattern of the $Bi_{0.13}Ca_{0.87}MnO_3$ sample. A comparison of the peak angles in the XRD pattern of this sample with those of $CaMnO_3$ showed that the crystal lattice was expanded by approximately 1% (from 3.729 A to 3.765 A – assuming pseudo-cubic). This expansion was attributed to the larger ion radius of Bi than Ca. $Bi_xCa_{1-x}MnO_3$ with x = 0.12~0.16 is orthorhombic and becomes triclinic with increasing Bi content. However, pseudo-cubic approximation is applicable because the orthorhombic deviation is small.

All other samples with different Bi contents showed similar patterns with minute differences. There were three peaks not related to the optimistic crystal structure (after reviewing JCPDS 3-0830 and 45-1266). These peaks are indicated by the arrow and 'x' in the Fig. 1, and are not related to any known crystal structures of $CaCO_3$, $Bi_2O_3$ or bismuth manganese oxide (BMO). They may belong to an unknown compound of bismuth calcium manganese oxide (BCMO).

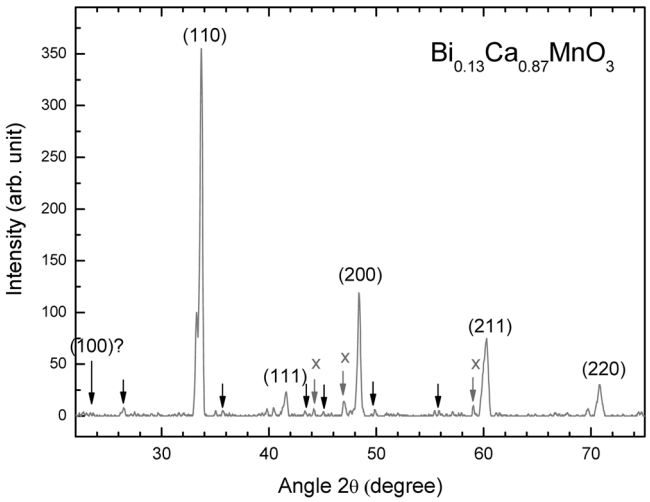


**Fig. 1.** XRD pattern of the $Bi_{0.13}Ca_{0.87}MnO_3$ sample: index based on the pseudocubic approximation. Small peaks indicated by the arrows are minor peaks associated with the structure, as in the JCPDS 3-0830. Three minor peaks indicated by the arrow and x are not associated with the other major peaks.

Fig. 2 shows the magnetic susceptibilities measured for the five $Bi_xCa_{1-x}MnO_3$ samples. The features of the magnetic susceptibility of each sample measured under a weak field (100 Oe) and strong field (3000 Oe) are somewhat different. Generally the weak field susceptibility is larger and show sharper peaks as a function of temperature. However, the main peaks around 115~125 K in the weak field measurement (left panel) are not altered significantly in the strong field measurements (right panel) for x = 0.12~0.14. Woo *et al.* [1] classified $Bi_xCa_{1-x}MnO_3$ with x in this range as a 'paramagnetic with ferromagnetic fluctuation' for high temperature. They coined the term 'anti-ferromagnetic charge ordered state' for $Bi_xCa_{1-x}MnO_3$ in temperature lower than the Neel temperature and for Bi content x > 0.14. Their phase diagram was based on the pre-existing studies plus their sparse experiments. A close examination clearly showed a change in the magnetic susceptibility due to variations in temperature and Bi content (x) over the range x = 0.12~0.16. Nevertheless, Woo *et al*. [1] and Chiba *et al.* [2] yielded fairly good estimates of the Neel temperature curve as a function of temperature and Bi content despite their limited number of samples (their sample Bi content interval was 3~5 times wider than ours).

The highest peaks in the magnetic susceptibility curves correspond to the Neel temperatures of the $Bi_xCa_{1-x}MnO_3$ samples. The Neel temperatures of these samples increase gradually with small increases in Bi content. However,

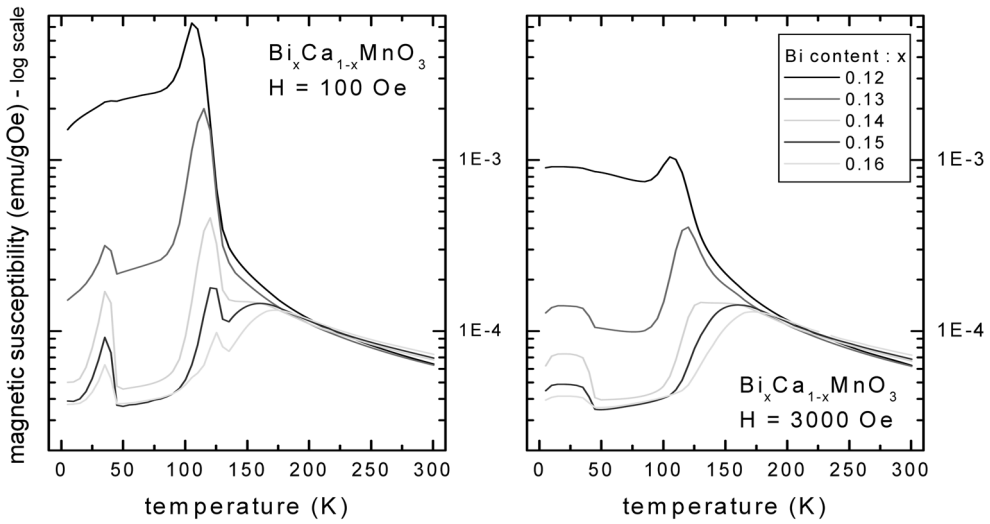


**Fig. 2.** Magnetic susceptibilities of the $Bi_xCa_{1-x}MnO_3$ samples measured at 100 Oe and 3000 Oe (temperature raised slowly from 5 K to 300 K).

the Neel temperatures could not be identified as clearly in the strong field susceptibilities as they could be in the weak field susceptibilities. Three peaks were observed in the weak field susceptibilities for the samples with x = 0.15 and 0.16. It is possible that a strong field (3000 Oe) induces the low spin states of manganese ions in these samples at low temperature range (T < 150 K).

There is a common ferromagnetic peak below T ~ 45 K for the four samples with x = 0.13~0.16 (the sample with x = 0.12 shows a very small trace only). It is possible that a secondary phase of BCMO, though in small quantities (minor peaks pointed with arrow and 'x' in the x-ray diffraction pattern - Fig. 1), becomes ferromagnetic below 45 K. The high magnetic susceptibility range of temperature is wider for a strong field measurement, possibly due to the strong field suppression of the low spin state. In the higher temperature range (T > 50 K), the unknown secondary phase would not significantly affect the overall magnetic and physical characteristics of these samples.

The weak field susceptibility of the samples with x = 0.16 and 0.15 show third peaks at approximately 160 K and 170 K. It is believed that these temperatures are associated with charge ordering, which was identified in BCMO by Woo *et al.* [1]. The temperatures determined by a closer examination of these magnetic susceptibility curves are shown in the Table 1. $Bi_xCa_{1-x}MnO_3$ showed charge ordering at Bi content x > 0.14 and the charge ordering temperature of $Bi_{x0.14}Ca_{0.86}MnO_3$ was determined to be 152 K.

A set of preliminary continous wave EMR experiments for the $Bi_xCa_{1-x}MnO_3$ samples was carried out. The signal line-width increased almost linearly with temperature for T > 140 K. This type of temperature dependence is different from that of semiconductor [7] and reflects the existence of itinerant electrons. The line-width was larger for samples with a lower Bi content. There was a overturn at T ~ 130 K in the EMR line-width of the sample with x = 0.12 and 0.13. Details of the EMR characteristics will be reported in a separate article.

**Table 1.** Three peaks in the weak field magnetic susceptibility of $Bi_xCa_{1-x}MnO_3$.

| Bi content | 1st peak onset | 2nd peak center | 3rd peak center |
|---|---|---|---|
| 0.12 | Small trace | 107 K | Not existent |
| 0.13 | 42 K | 114 K | Not existent |
| 0.14 | 44 K | 119 K | 152 K |
| 0.15 | 43 K | 122 K | 161 K |
| 0.16 | 44 K | 126 K | 171 K |

Fig. 3 shows the resistivity of the $Bi_xCa_{1-x}MnO_3$ samples with x = 0.13 and 0.15. The resistivity of the samples increased slightly with increasing temperature. The two arrows in Fig. 3 indicate the Neel temperatures of the two samples identified from the magnetic susceptibility curves, and they are near the maximum slope in the curves.

The temperature dependence of the two $Bi_xCa_{1-x}MnO_3$ samples are in accordance with the other resistivity measurements of the former studies [1, 3]. Indeed, preliminary resistivity measurements of all five samples show the same gradual change according to the Bi content. In addition, the resistivity variations matched the EMR line-width variations because the existence of itinerant electrons reduces the resistivity and increases the EMR line-width.

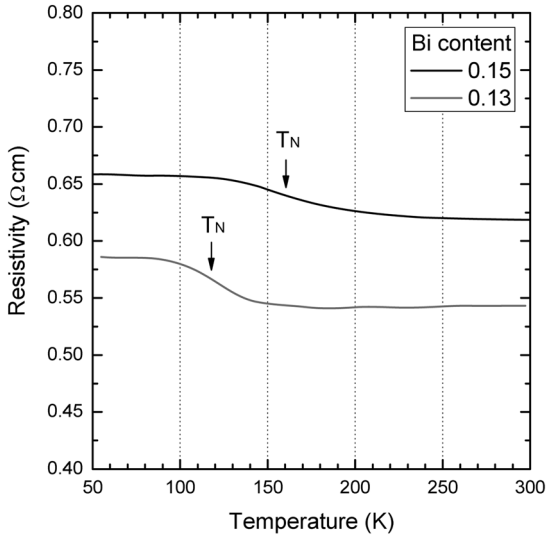


**Fig. 3.** Resistivity of $Bi_xCa_{1-x}MnO_3$ with x = 0.13 and 0.15.

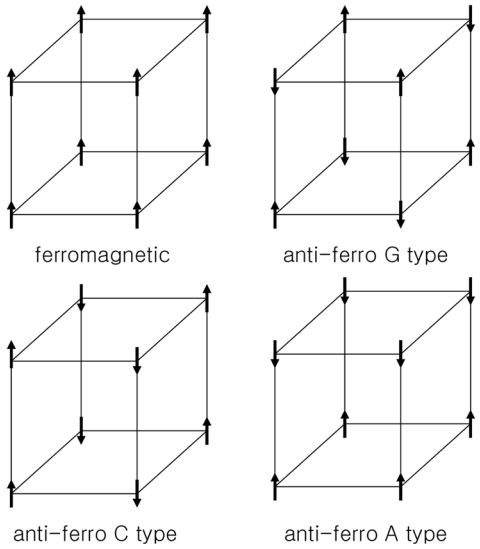


**Fig. 4.** Schematic diagram of the magnetic ordering for ferromagnetic and anti-ferromagnetic phases of BCMO.

The total energy, density of states and spin magnetic moments of the different magnetic phases of $Bi_xCa_{1-x}MnO_3$ were evaluated by first principles calculations based on the density functional theory. First, a local spin density approximation (LSDA) for the exchange and correlation energy term was used in the calculation. The projection augmented wave (PAW) pseudopotentials were used in all calculations [8]. The energy-cutoff was assigned to 400 eV. The Monkhorst-Pack method was used to choose the k-points. And, the grid number of k-points used were (3, 3, 3). The calculations were carried out for cells of $Bi_xCa_{1-x}MnO_3$ with six different values of x: x = 0, 0.125, 0.25, 0.5, 0.75, and 1. The simulated unit cells were designed as a cubic crystal with a lattice parameter ranging from 3.739 to 3.790 A, which increases linearly with increasing Bi content. Each cell was composed of 40 ions - 8 Bi or Ca ions, 8 Mn ions, and 24 O ions. The average electronic valence of the manganese ions in the cell varies from 4+ ~ 3+ and the corresponding spin magnetic moment of Mn ions (high spin) varies from 1.5 ~2.0 accordingly (valence: y = 4 – x, spin: s = 1.5 + 0.5 x, where x stands for the Bi content and spin is in the unit of Bohr magneton $\mu_B$).

For each of the six cases, all possible Bi and Ca ions configurations were considered so that the ensemble average could be attained. For example, there are three different configurations for the cases with a Bi content of 0.25. However, the stability of these different configurations was later found to be similar. For every ion cell configuration, the main three types - A, G, and C anti-ferromagnetic states and ferromagnetic state were considered (Fig. 4). Since the samples prepared and studied in the experimental part of this study have a Bi content of 0.12~0.16, the theoretical consideration of this study also concentrated on $Bi_xCa_{1-x}MnO_3$ with x = 0.125, 0.25, and 0.

The stable magnetic phases of the $Bi_xCa_{1-x}MnO_3$ with all three values of x were found to be anti-ferromagnetic according to the LSDA calculations. Although the calculated total energy was lower for the ferromagnetic

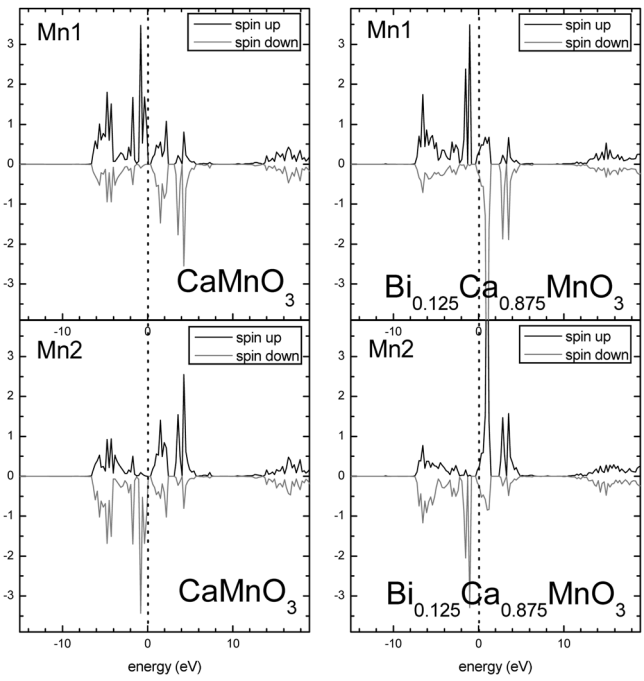


**Fig. 5.** Electronic density of states of two adjacent Mn ions in $CaMnO_3$ and $Bi_{0.125}Ca_{0.875}MnO_3$ in the relatively stable magnetic phase (G-type anti-ferromagnetic) – LSDA calculation (density of states scale = number of states per unit cell).

**Table 2.** Stable Magnetic Phases Predicted by First Principles Calculation.

| | LSDA | LSDA+U (3 eV) | LSDA+U (5 eV) |
|---|---|---|---|
| $Bi_{0.25}Ca_{0.75}MnO_3$ | AF(A) = AF(C) | AF(A), FM | FM, AF(A) |
| $Bi_{0.125}Ca_{0.875}MnO_3$ | AF(C), AF(G) | AF(C), AF(A) | AF(A), AF(C)=FM |
| $CaMnO_3$ | AF(G), AF(C) | AF(G), AF(C) | AF(C), AF(G) |

phase of a compound with x = 0.75 and 1 in the case of no relaxation, the anti-ferromagnetic phases were more stable when the ion positions were relaxed. Therefore, it is confirmed that the displacements of the ions, so called Jahn-Teller distortion, is associated with the anti-ferromagnetic ordering in these compounds. Fig. 5 shows the calculated electronic density of states of the two adjacent manganese ions of $Bi_xCa_{1-x}MnO_3$ with x = 0 and 0.125. The magnetic moments of the adjacent manganese ions are opposite to each other, which would cancel out the macroscopic magnetic moments of the compounds. In addition, the calculated magnetic moments of manganese ions were 2.487, 2.549~2.552 and 2.612~2.628 $\mu_B$ for $Bi_xCa_{1-x}MnO_3$ with x = 0, 0.125 and 0.25, respectively. These are comparable to the values in former studies [6]. In the figure, the dotted lines indicate the Fermi energy level. In addition, $Bi_{0.125}Ca_{0.875}MnO_3$ is expected to have a higher conductivity than $CaMnO_3$ because more states exist at the Fermi energy level in the former - $Bi_{0.125}Ca_{0.875}MnO_3$.

LSDA calculations are generally successful in predicting the ground states of solid states. However, these calculations often fail to do so, particularly for strongly correlated materials. For those cases, LSDA+U is known to have better performance and was also attempted in this study. U, which refers to the on-site Coulomb interaction energy, is taken to be 3 and 5 eV for the 4d orbital electron of Bi and the 3d orbital electron of Mn. All other calculation schemes and parameters assigned in the LSDA+U calculations were the same as in the LSDA calculations.

While LSDA predicted the C type and G type anti-ferromagnetic state to be more stable than the A type or ferromagnetic state for $Bi_{0.125}Ca_{0.875}MnO_3$, LSDA+U predicts the A type anti-ferromagnetic to be most stable. LSDA predicted A type and C type to be the most stable for $Bi_{0.25}Ca_{0.75}MnO_3$. However, LSDA+U predicted the ferromagnetic state to be more stable than all types of anti-ferromagnetic states (A type only be competitive) when U was taken as 5 eV. Some intermediate prediction is made with U taken as 3 eV. In addition, the G type anti-ferromagnetic state was most unfavorable for both $Bi_{0.125}Ca_{0.875}MnO_3$ and $Bi_{0.25}Ca_{0.75}MnO_3$ according to LSDA+U calculation (U be either 3 or 5 eV).

Table 2 lists the 1st and 2nd stable magnetic phase of $Bi_xCa_{1-x}MnO_3$ with x = 0, 0.125, and 0.25 predicted by LSDA and LSDA+U (U = 3 or 5 eV). According to the table, the stability of each magnetic phase is quite competitive. The total energy difference E[AF(G)] – E[AF(C)] calculated in this study for $CaMnO_3$ for the three cases were –30, –21, +17.5 meV, while –59 or –39 meV was predicted in another study [6]. All the total energy differences calculated in this study are listed in the appendix.

The anti-ferromagnetic characteristics of $Bi_xCa_{1-x}MnO_3$ were confirmed in both the magnetic susceptibility curve and first principle calculations. The relative stability between the anti-ferromagnetic phases is different for the LSDA and LSDA+U calculations. Even a ferromagnetic phase was predicted for $Bi_{0.25}Ca_{0.77}MnO_3$ when the onsite Coulomb energy was assigned to 5 eV. The high magnetic susceptibility of $Bi_{0.12}Ca_{0.88}MnO_3$ at low temperatures may be due to the coexistence of a ferromagnetic phase in the anti-ferromagnetic phase. The same hypothesis may hold for other $Bi_xCa_{1-x}MnO_3$ samples. It is believed that the difference in cooling or other sample preparation process can result in different magnetic phases of the final samples of $Bi_xCa_{1-x}MnO_3$ with x = 0.125~0.25.

## 4. Conclusion

The magnetic characteristics and other physical properties were investigated experimentally for $Bi_xCa_{1-x}MnO_3$ with Bi content x = 0.12~0.16. In addition, first principles calculations of their magnetic phase stability were carried for $Bi_xCa_{1-x}MnO_3$ with Bi content x = 0, 0.125, and 0.25. The anti-ferromagnetic characteristics of the samples were confirmed by the magnetic susceptibility measurements. The Neel temperature of each sample was also identified from those curves. The Neel temperatures and charge ordering temperatures were identified more accurately than in previous studies. The resistivity and EMR experiments partly revealed the physical properties of $Bi_xCa_{1-x}MnO_3$ with x = 0.12~0.16. In addition, it was confirmed that those properties are in accordance with the magnetic susceptibility measurements and also with the previous studies.

The anti-ferromagnetic characteristics of $Bi_xCa_{1-x}MnO_3$ is not genuine but is overlapped with charge ordering for

Bi content x = 0.14~0.16. Moreover, the high magnetic susceptibility at low temperatures was confirmed, particularly for the sample with x = 0.12. The results of first principles calculations predict anti-ferromagnetic phase of $Bi_xCa_{1-x}MnO_3$ with x = 0, 0.125, and 0.25 but predict the ferromagnetic phase to be almost equally or slightly less stable.

## Acknowledgement

This study was partly supported by KRF-2006-005-J02804. The authors are grateful to Dr. C. H. Park for advice in the first principles calculation and Dr. Y. C. Kim for allowance to use facilities for the sample preparation. Dr. J. S. Ahn gave help discussing the sample preparation. Careful review of unknown referees and text grammar check of native editor are appreciated. Finally the first author would like to acknowledge the Heavenly helps for this study.

## References

[1] H. Woo, T. A. Tyson, M. Croft, S.-W. Cheong, and J. C. Woicik, Phys. Rev. B **63**, 134412 (2001).
[2] H. Chiba, T. Atou, H. Faqir, M. Kikuchi, Y. Syono, Y. Murakami, and D. Shindo, Sol. St. Ion. **108**, 193 (1998).
[3] H. Chiba, M. Kikuchi, K. Kusaba, Y. Muraoka, and Y. Syono, Sol. St. Com. **99**, 499 (1996).
[4] S. H. Na, J. W. Kim, S. N. Choi, and J. W. Park, J. Magnetics **11**, 95 (2006).
[5] J. H. Park, S. K. Kwon, and B. I. Min, J. Magnetics **12**, 64 (2007).
[6] M. Nicastro, M. Kuzmin, and C. H. Patterson, Com. Mat. Sc. **17**, 445 (2000).
[7] S. H. Na, H. C. Kim, J. W. Park, and J. W. Kim, J. Magnetics **13**, 23 (2008).
[8] G. Kresse and J. Joubert, Phys. Rev. B **59**, 1758 (1999).

## Appendix

Table of the Calculated Total Energy Differences of the Four Magnetic Phases of $Bi_xCa_{1-x}MnO_3$ with x = 0, 0.125, and 0.25 predicted by LSDA and LSDA+U (U = 3 or 5 eV). (The energy values are referenced to the most stable magnetic phase and are scaled to one Mn ion)

**$CaMnO_3$**

| LSDA | | LSDA+U(3) | | LSDA+U(5) | |
|---|---|---|---|---|---|
| **AF(G)** | 0 meV | **AF(G)** | 0 meV | **AF(C)** | 0 meV |
| AF(C) | +30 meV | AF(C) | +21 meV | AF(G) | +18 meV |
| AF(A) | +84 meV | AF(A) | +43 meV | AF(A) | +32 meV |
| FM | +980 meV | FM | +68 meV | FM | +32 meV |

**$Bi_{0.125}Ca_{0.875}MnO_3$**

| LSDA | | LSDA+U(3) | | LSDA+U(5) | |
|---|---|---|---|---|---|
| **AF(C)** | 0 meV | **AF(C)** | 0 meV | **AF(A)** | 0 meV |
| AF(G) | +6 meV | AF(A) | +5 meV | AF(C) | +12 meV |
| AF(A) | +35 meV | FM | +31 meV | FM | +12 meV |
| FM | +96 meV | AF(G) | +43 meV | AF(G) | +93 meV |

**$Bi_{0.25}Ca_{0.75}MnO_3$**

| LSDA | | LSDA+U(3) | | LSDA+U(5) | |
|---|---|---|---|---|---|
| **AF(A)** | 0 meV | **AF(A)** | 0 meV | **FM** | 0 meV |
| AF(C) | +2 meV | FM | +7 meV | AF(A) | +6 meV |
| AF(G) | +28 meV | AF(C) | +35 meV | AF(C) | +54 meV |
| FM | +48 meV | AF(G) | +119 meV | AF(G) | +190 meV |